

## Design of reversible organic–organometallic multi-redox systems using thianthrene having ferrocene fragments

Satoshi Ogawa,\* Hiroki Muraoka and Ryu Sato\*

Department of Chemical Engineering, Faculty of Engineering, Iwate University, Morioka 020-8551, Japan

Received 19 January 2006; revised 9 February 2006; accepted 13 February 2006

Available online 28 February 2006

**Abstract**—1-Ferrocenyl- and 1,9-diferrocenyl-thianthrenes have been synthesized by using palladium-catalyzed cross-coupling reactions of 1-bromo- and 1,9-dibromo-thianthrenes with ferrocenylzinc chloride. The structure of 1-ferrocenylthianthrene was determined by X-ray crystallographic analysis. 1-Ferrocenyl- and 1,9-diferrocenyl-thianthrenes show well-defined separated two-steps two-electrons and three-steps three-electrons reversible redox waves derived from the ferrocenium cation and the thianthrene radical cation, respectively, by the cyclic voltammetry in dichloromethane containing the supporting electrolyte anion of  $[\text{B}(\text{C}_6\text{F}_5)_4]^-$ . © 2006 Elsevier Ltd. All rights reserved.

Molecules comprising multiple reduction–oxidation (redox) centers have received much attention in recent years due to the preparation of new organic semiconducting materials with application in material science.<sup>1</sup> Moreover, this kind of molecule having two or more redox-active metal centers is a fundamentally interesting attractive target for the study of multi-electron transfer processes via the mixed valence state derived from these multi-metallic systems.<sup>2</sup> Our interest in the design of reversible multi-redox systems containing both organic and organometallic fragments in one molecule prompted us to synthesize functionalized thianthrenes containing organometallic fragments. Thianthrene with  $\pi$ -donor properties is an expected central organic unit for the construction of a new type of donor system from the following viewpoint of structural and redox properties:<sup>3</sup> (1) oxidation of thianthrene to the  $7\pi$  radical cation species occurs reversibly; (2) the thianthrene radical cation is thermodynamically stable; (3) oxidation of thianthrene converts a neutral bent structure to a planar radical cation structure and (4) thianthrene and oxidized thianthrene units form highly ordered arrays with intermolecular interactions involving both  $\pi$ – $\pi$  stacking and S–S contacts. However, there is no report concerning a donor system based on functionalized thianthrene, which is of structural and redox characteristic interest,

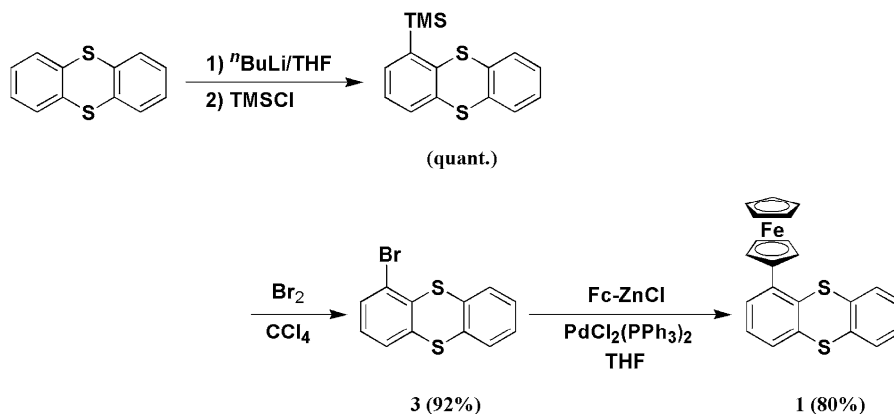
in contrast to a donor system based on tetrathiafulvalene (TTF) with  $\pi$ -donor property as well as thianthrene. Previously, it was reported that a donor system consisting of TTF and ferrocene, which is known as a famous metallocene with donor properties, showed a multi-steps multi-electrons reversible redox wave corresponding to oxidation of TTF and ferrocene in their cyclic voltammograms.<sup>4</sup> Therefore, we have designed 1-ferrocenyl- and 1,9-diferrocenyl-thianthrenes as organic–organometallic hybrid molecules. In this letter, we report the synthesis, structural characterization, and electrochemical properties of 1-ferrocenyl- and 1,9-diferrocenyl-thianthrenes (**1** and **2**).

The synthesis of two target molecules, **1** and **2**, was established by the use of typical transition-metal catalyzed cross-coupling reactions as follows (Schemes 1 and 2). The reaction of ferrocene in tetrahydrofuran (THF) with *tert*-butyllithium at 0 °C followed by treatment with  $\text{ZnCl}_2$  at room temperature produced ferrocenylzinc chloride. The cross-coupling reactions of 1-bromo- and 1,9-dibromo-thianthrenes (**3** and **4**), which were prepared by the modified methods previously reported,<sup>5</sup> with ferrocenylzinc chloride in the presence of catalytic amounts of  $\text{PdCl}_2(\text{PPh}_3)_2$  in THF under reflux conditions gave **1** and **2** in 80% and 71% isolated yields, respectively.<sup>6</sup>

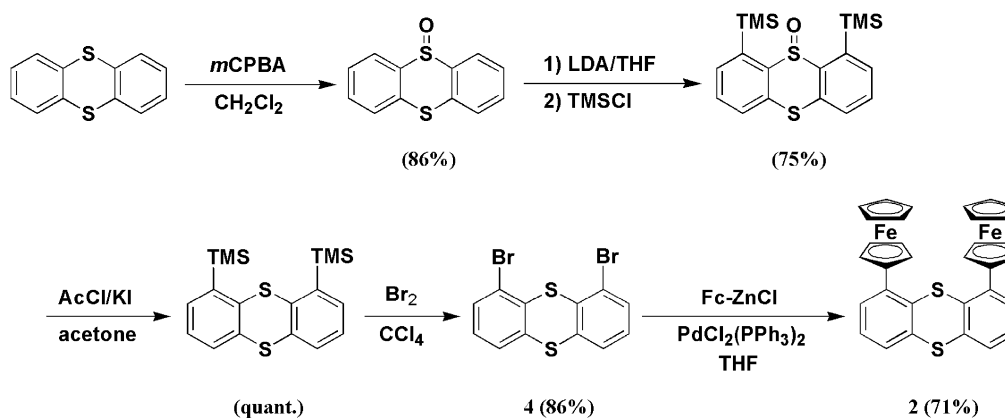
The crystal structure of **1** was confirmed by X-ray crystallographic analysis (Fig. 1).<sup>7</sup> The butterfly angle between the two benzene rings (wings) of the thianthrene

**Keywords:** Ferrocene; Thianthrene; Cyclic voltammetry; Redox reaction.

\*Corresponding authors. Tel./fax: +81 19 621 6934 (S.O.); e-mail: [ogawa@iwate-u.ac.jp](mailto:ogawa@iwate-u.ac.jp)



Scheme 1.



Scheme 2.

is  $129.4^\circ$ , which is in good agreement with the typical value of  $128^\circ$  for the previously reported parent thianthrene.<sup>3a,8</sup> The substituted cyclopentadienyl ring is rotated  $139^\circ$  from the benzene ring, and the C–C distance between the ferrocenyl and benzene groups suggests a double bond character because the length of  $1.479(2)$  Å is slightly shorter than that of the  $sp^2$ – $sp^2$  single bond ( $1.516$  Å). The crystal packing reveals that two molecules form  $\pi$ -stacked structure between substituted benzene rings (Fig. 2). The  $\pi$ – $\pi$  interaction distance ( $3.651(10)$  Å) between the least-squares plane centers is similar to that of standard thianthrene  $\pi$ – $\pi$  stacking.

The redox properties of thianthrene–ferrocene systems have been furnished by electrochemical measurements; the data are collected in Table 1 and cyclic and differential pulse voltammograms of compounds **1** and **2** are shown in Figure 3. The cyclic voltammograms of compounds **1** and **2** measured in dichloromethane ( $\text{CH}_2\text{Cl}_2$ ) containing  $0.1 \text{ mol dm}^{-3}$   $[\text{Bu}_4\text{N}]^+[\text{PF}_6]^-$  as a supporting electrolyte showed two one-electron oxidation processes and three one-electron oxidation processes corresponding to ferrocene and thianthrene moieties as judged by their respective differential pulse voltammograms. Oxidation behavior of **1** is a well-defined reversible first wave derived from the ferrocenium cation, but precipitation of the dication radical generated by subsequent one-electron oxidation of the thianthrene fragment and

cathodic stripping wave on the return sweep is observed. On the other hand, oxidation behavior of **2** is both reversible through the closely spaced first and second waves which reflected the weak interaction of the intramolecular two ferrocenyl groups, and the stripping-type third wave derived from the trication radical is observed in a similar manner of compound **1**. These results clearly indicate that the produced multiply-charged cation radicals are not sufficiently soluble in  $\text{CH}_2\text{Cl}_2$  due to its low polarity.

On the other hand, recently, it has been reported that cyclic voltammetry in  $\text{CH}_2\text{Cl}_2$  solution containing  $[\text{Bu}_4\text{N}]^+[\text{B}(\text{C}_6\text{F}_5)_4]^-$  as a supporting electrolyte gives enhanced behavior for oxidation of complexes containing two or more ferrocenyl groups, owing to good stability and solubility of the multiply-charged oxidation products.<sup>9</sup> We employed this electrochemical technique, and the cyclic voltammograms obtained for compounds **1** and **2** are shown in Figure 4. By employing  $0.05 \text{ mol dm}^{-3}$   $[\text{Bu}_4\text{N}]^+[\text{B}(\text{C}_6\text{F}_5)_4]^-$  as a supporting electrolyte in  $\text{CH}_2\text{Cl}_2$ , all oxidation waves derived from the ferrocenium cation and thianthrene radical cation showed good separated and well-defined reversible redox couples. These results clearly indicate that all oxidation species are stable in fully soluble state. In addition, the difference between the first and second half-potentials ( $\Delta E_{1/2} = E_{1/2}^1 - E_{1/2}^2$ ) for the Fe(II)–Fe(III) and

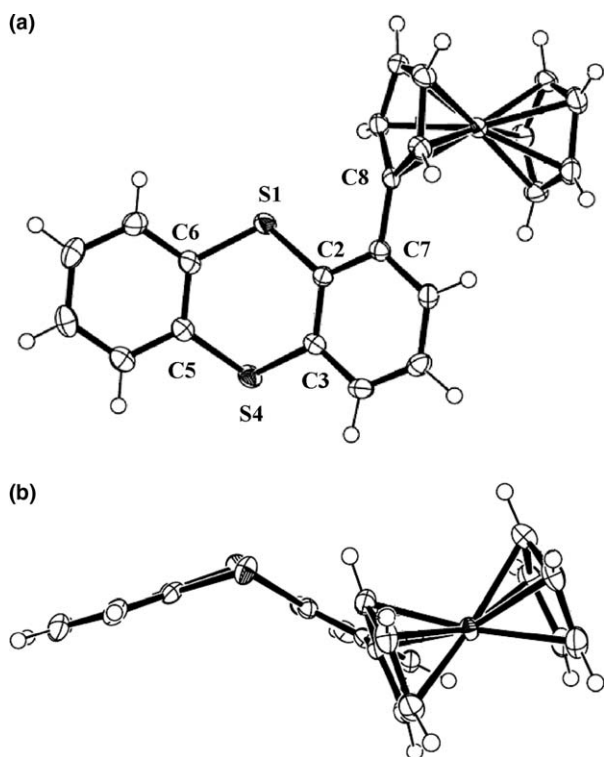


**Figure 1.** (a) ORTEP drawing of **1**. Thermal ellipsoids are drawn at 50% probability. Selected bond lengths (Å) and bond angles (°): S1–C2 1.7762(16), C2–C3 1.398(2), C3–S4 1.7697(17), S4–C5 1.7653(18), C5–C6 1.387(2), C7–C8 1.479(2), S1–C2–C3 119.71(12), C2–C3–S4 121.33(12), C3–S4–C5 101.53(7), S4–C5–C6 120.21(13), C5–C6–S1 121.52(13), C6–S1–C1 102.45(8). (b) Side view of **1**.

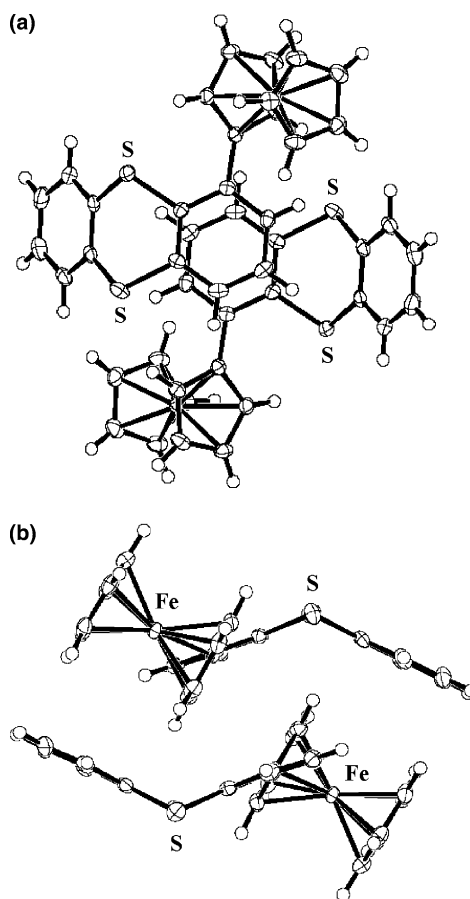


**Figure 2.** Top (a) and side (b) view of  $\pi$ -stacked structure of **1**.

Fe(III)–Fe(III) couples of **2** when the counter-anion was replaced from  $[\text{PF}_6]^-$  to  $[\text{B}(\text{C}_6\text{F}_5)_4]^-$  increases from 73 to 178 mV, which gave comproportionation constants  $K_c = 18$  and  $1.2 \times 10^3$  for the Fe(II)–Fe(III) mixed-valence state, respectively. These results suggest that the thermodynamic stabilization of **2** arises from enhancement of the electronic interaction between the metal center of ferrocene and the ferrocenium cation in the mixed-valence state owing to diminishing ion-pairing interaction of the  $\text{Fe}^{\text{III}}$  center with the borate anion with four

**Table 1.** Redox potentials [V vs  $\text{Ag}/\text{Ag}^+$ ]

	<b>1</b>		<b>2</b>		
	First	Second	First	Second	Third
$E_{\text{pa}}$	+0.34	+1.25	+0.30 <sup>b</sup>	+0.37	+1.32
$E_{\text{pc}}$	+0.22	+1.10 <sup>a</sup>	+0.22	+0.31 <sup>b</sup>	+1.17 <sup>a</sup>
$E_{1/2}$	+0.28	—	+0.26 <sup>b</sup>	+0.34 <sup>b</sup>	—

<sup>a</sup> Stripping-type waves.

<sup>b</sup> Calculated using peak potentials of DPV.

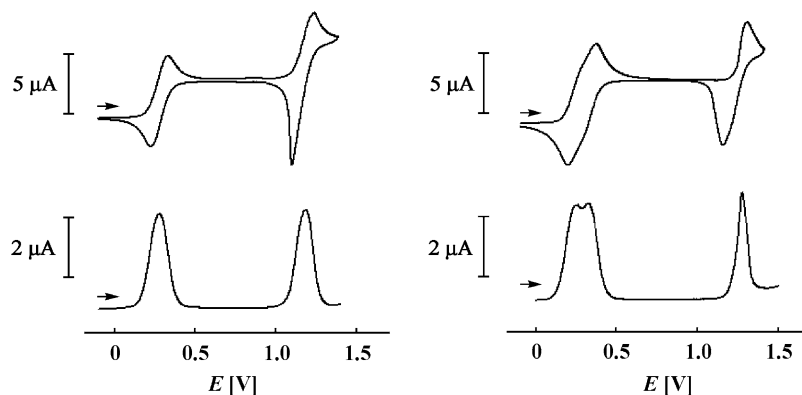


**Figure 3.** Cyclic (top) and differential pulse (bottom) voltammograms of **1** (left) and **2** (right) in  $2 \text{ mmol dm}^{-3}$   $\text{CH}_2\text{Cl}_2$  solution containing  $0.1 \text{ mol dm}^{-3}$   $[\text{Bu}_4\text{N}]^+[\text{PF}_6]^-$  using a glassy-carbon working electrode and  $\text{Ag}/0.01 \text{ mol dm}^{-3}$   $\text{AgNO}_3$  in  $0.1 \text{ mol dm}^{-3}$   $[\text{Bu}_4\text{N}]^+[\text{PF}_6]^-/\text{CH}_3\text{CN}$  solution as a reference electrode; scan rate was  $100 \text{ mV s}^{-1}$ .

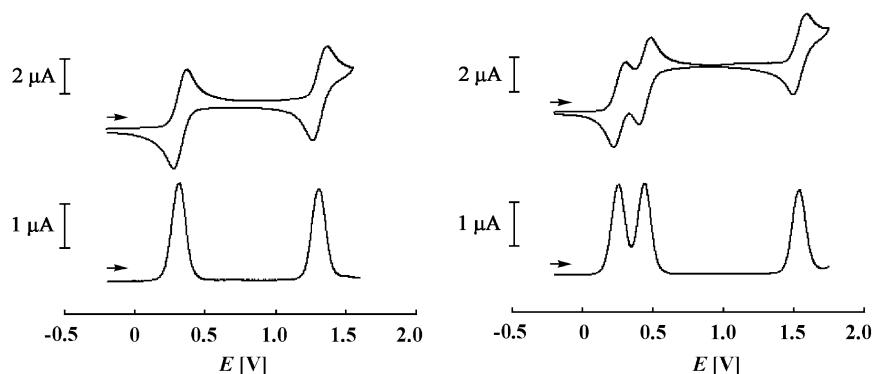


**Figure 4.** Cyclic (top) and differential pulse (bottom) voltammograms of **1** (left) and **2** (right) in 1 mmol dm<sup>-3</sup> CH<sub>2</sub>Cl<sub>2</sub> solution containing 0.05 mol dm<sup>-3</sup> [Bu<sub>4</sub>N]<sup>+</sup>[B(C<sub>6</sub>F<sub>5</sub>)<sub>4</sub>]<sup>-</sup> using a glassy-carbon working electrode and Ag/0.01 mol dm<sup>-3</sup> AgNO<sub>3</sub> in 0.05 mol dm<sup>-3</sup> [Bu<sub>4</sub>N]<sup>+</sup>[B(C<sub>6</sub>F<sub>5</sub>)<sub>4</sub>]<sup>-</sup>/CH<sub>3</sub>CN solution as a reference electrode; scan rate was 100 mV s<sup>-1</sup>.

**Table 2.** Redox potentials [V vs Ag/Ag<sup>+</sup>]

	<b>1</b>		<b>2</b>		
	First	Second	First	Second	Third
$E_{pa}$	+0.37	+1.37	+0.30	+0.48	+1.59
$E_{pc}$	+0.28	+1.27	+0.23	+0.40	+1.50
$E_{1/2}$	+0.33	+1.32	+0.27	+0.44	+1.55

bulky and electron-withdrawing pentafluorophenyl moieties (compared with hexafluorophosphate), which leads  $E_{1/2}^2$  to shift to more positive (anodic) potentials (Table 2).

In conclusion, we have synthesized 1-ferrocenyl- and 1,9-diferrocenyl-thianthrenes by palladium-catalyzed cross-coupling reactions. The crystal structure of **1** was confirmed by X-ray crystallographic analysis. The electrochemical properties of **1** and **2** were furnished by cyclic and differential pulse voltammetric studies. When a weak ion-pairing anion [B(C<sub>6</sub>F<sub>5</sub>)<sub>4</sub>]<sup>-</sup> was employed as a supporting electrolyte in CH<sub>2</sub>Cl<sub>2</sub>, the cyclic voltammograms showed reversible multi-electron transfer phenomena assigned to ferrocene (organometallic) and thianthrene (organic) fragments owing to good stability and solubility of the multiply-charged oxidation products. Therefore, we succeeded in establishing a new type of multi-steps reversible redox systems using organic-organometallic hybrid molecules.

#### Acknowledgements

This work was supported by Grant-in-Aid for Scientific Research (No. 15550023) from the Ministry of Education, Culture, Sports, Science and Technology. We thank Ms. Shiduko Nakajo (Division of Elemental Analysis, Iwate University) for elemental analyses.

#### Supplementary data

Supplementary data associated with this article can be found, in the online version, at doi:10.1016/j.tetlet.2006.02.062.

#### References and notes

- (a) Iyoda, M.; Hasegawa, M.; Miyake, Y. *Chem. Rev.* **2004**, *104*, 5058–5113; (b) Fichou, D. *Handbook of Oligo- and Polythiophenes*; VCH: Weinheim, 1999; (c) Martin, N.; Sánchez, L.; Illescas, B.; Pérez, I. *Chem. Rev.* **1998**, *98*, 2527–2547.
- (a) Hamaguchi, T.; Nagano, H.; Hoki, K.; Kido, H.; Yamaguchi, T.; Breedlove, B. K.; Ito, T. *Bull. Chem. Soc. Jpn.* **2005**, *78*, 591–598; (b) Nishihara, H. *Bull. Chem. Soc. Jpn.* **2001**, *74*, 19–29; (c) Barlow, S.; O'Hare, D. *Chem. Rev.* **1997**, *97*, 637–669.
- (a) Bock, H.; Rauschenbach, A.; Näther, C.; Kleine, M.; Havlas, Z. *Chem. Ber.* **1994**, *127*, 2043–2049; (b) Stender, K.-W.; Klar, G. *Z. Naturforsch.* **1985**, *40b*, 774–781.
- For a recent review, see: Sarhan, A. A. O. *Tetrahedron* **2005**, *61*, 3889–3932, and references cited therein; especially, Iyoda, M.; Takano, T.; Otani, N.; Ugawa, K.; Yoshida, M.; Matsuyama, H.; Kuwatani, Y. *Chem. Lett.* **2001**, 1310–1311; Moore, A. J.; Skabara, P. J.; Bryce, M. R.; Batsanov, A. S.; Howard, J. A. K.; Daley, S. T. A. K. *J. Chem. Soc., Chem. Commun.* **1993**, 417–418.
- (a) Lovell, J. M.; Beddoes, R. L.; Joule, J. A. *Tetrahedron* **1996**, *52*, 4745–4756; (b) Furukawa, N.; Kimura, T.; Horie, Y.; Ogawa, S. *Heterocycles* **1991**, *32*, 675–678.
- Spectral and physical data for **1**: orange crystals; mp 162.2–163.0 °C (decomp.); <sup>1</sup>H NMR (400 MHz, CDCl<sub>3</sub>) δ 4.16 (s, 5H, *free*-Cp), 4.38 (t, *J* = 1.8 Hz, 2H, C<sub>5</sub>H<sub>4</sub>), 4.70 (t, *J* = 1.8 Hz, 2H, C<sub>5</sub>H<sub>4</sub>), 7.16–7.25 (m, 3H, ArH), 7.40 (dd, *J* = 1.3, 7.6 Hz, 1H, ArH), 7.47 (dd, *J* = 1.6, 7.5 Hz, 1H, ArH), 7.48 (dd, *J* = 1.6, 7.5 Hz, 1H, ArH), 7.66 (dd, *J* = 1.3, 7.6 Hz, 1H, ArH); <sup>13</sup>C NMR (101 MHz, CDCl<sub>3</sub>) δ 68.3, 69.7, 70.6, 85.9, 126.7, 127.1, 127.5, 127.8, 128.4, 128.8, 130.1, 135.05, 135.11, 136.0, 136.6, 139.1, 139.18; IR (KBr) ν 3084, 1574, 1427, 1253, 1107, 1001, 789, 744, 484 cm<sup>-1</sup>; MS (70 eV) *m/z* 400 (M<sup>+</sup>); Anal. Calcd for C<sub>22</sub>H<sub>16</sub>FeS<sub>2</sub>: C, 66.00; H, 4.03. Found: C, 66.22; H, 4.24. Spectral and physical data for **2**: orange crystals; mp >255 °C (decomp.); <sup>1</sup>H NMR (400 MHz, CDCl<sub>3</sub>) δ 4.13 (s, 10H, *free*-Cp), 4.30 (t, *J* = 1.8 Hz, 4H, C<sub>5</sub>H<sub>4</sub>), 4.57 (t, *J* = 1.8 Hz, 4H, C<sub>5</sub>H<sub>4</sub>), 7.20 (t, *J* = 7.7 Hz, 2H, ArH), 7.42 (dd, *J* = 1.2, 7.7 Hz, 2H, ArH), 7.64 (dd, *J* = 1.2, 7.7 Hz, 2H, ArH); <sup>13</sup>C NMR (101 MHz, CDCl<sub>3</sub>) δ 68.2, 69.5, 70.6, 85.8, 126.9 (2C), 129.8, 135.3, 137.2, 139.8; IR (KBr) ν 3093, 1578, 1381, 1105, 1001, 823, 764, 505, 490 cm<sup>-1</sup>; MS (70 eV) *m/z* 584 (M<sup>+</sup>); Anal. Calcd for C<sub>32</sub>H<sub>24</sub>Fe<sub>2</sub>S<sub>2</sub>: C, 65.77; H, 4.14. Found: C, 65.80; H, 4.34.
- Crystal data for **1**: *M* = 400.34, C<sub>22</sub>H<sub>16</sub>FeS<sub>2</sub>, monoclinic, space group *P*2<sub>1</sub>/*n* (no. 14), *a* = 10.0956(14) Å, *b* =

13.6838(14) Å,  $c = 12.3554(13)$  Å,  $\beta = 93.728(5)^\circ$ ,  $V = 1703.2(3)$  Å<sup>3</sup>,  $Z = 4$ ,  $D_{\text{calc}} = 1.561$  g/cm<sup>3</sup>,  $T = -123 \pm 1$  K,  $\lambda$  (MoK $\alpha$ ) = 0.71075 Å. 15763 reflections measured, 3872 unique ( $R_{\text{int}} = 0.034$ ).  $R = 0.0264$ ,  $R_w = 0.0513$  (on 3872 observed reflections [ $I > 2.00\sigma(I)$ ] and 290 variable parameters (CCDC 298079)).

8. Klar, G. In *Methods of Organic Chemistry*, 4th ed.; Schumann, E., Ed.; Thieme: Stuttgart, 1997; pp 250–407, Vol. Epa.
9. (a) Camire, N.; Mueller-Westerhoff, U. T.; Geiger, W. E. *J. Organomet. Chem.* **2001**, 637–639, 823–826; (b) LeSuer, R. J.; Geiger, W. E. *Angew. Chem., Int. Ed.* **2000**, 39, 248–250.